Fig. 3. Photoluminescence spectra of nanocrystalline GaN.

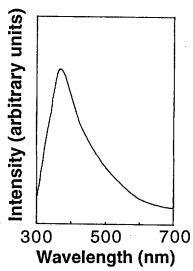

cell volume increases as pressure decreases; the lattice parameter was estimated to be 4.035 Å at 37 GPa.

Transmission electron microscopy (TEM) images were taken with a Hitachi H-800 transmission electron microscope. These crystallites of GaN have an average size of 32 nm and display a uniform shape (Fig. 2A). High-resolution electron microscopy (HREM) images of GaN particles were taken on a JEOL-2010 transmission electron microscope. In Fig. 2B, the (001) lattice fringes of GaN in the wurtzite structure appear frequently, indicating the preferential orientation of the platelike GaN particles. The areas marked by arrowheads (A and B) in Fig. 2C represent a typical structural image of [100] and [110] orientations, respectively, of GaN in the rocksalt structure.

Photoluminescence (PL) spectra of the nanocrystalline GaN were measured in a Hitachi 850 fluorescence spectrophotometer with a Xe lamp at room temperature. The excitation wavelength was 254 nm, and the filter wavelength was 310 nm. The PL spectrum (Fig. 3) consists of one broad emission feature at 370 nm, which is in agreement with that of the bulk GaN (*12*). This result indicates that the as-prepared GaN is too large for quantum confinement, and in fact the Bohr exciton radius for GaN is 11 nm, which could be calculated according to (*13*).

REFERENCES AND NOTES

1. R. Dingle and K. L. Shaklee, *Appl. Phys. Lett.* **19**, 5 (1971).
2. R. S. Schmitt *et al.*, *Phys. Rev. B* **35**, 8113 (1987).
3. H. Xia, Q. Xia, A. L. Ruoff, *ibid.* **47**, 12925 (1993).
4. W. C. Johnson, J. B. Parsons, M. C. Crew, *J. Phys. Chem.* **36**, 2561 (1932).
5. A. Addamiano, *J. Electrochem. Soc.* **108**, 1072 (1961); Z. A. Munir and A. W. Searcy, *J. Chem. Phys.* **42**, 4223 (1965); I. G. Pichugin and D. A. Searcy, *Inorg. Mater.* **6**, 1732 (1970); B. J. Isherwood and D. K. Wickenden, *J. Mater. Sci.* **5**, 869 (1970); E. Ejder, *J. Cryst. Growth* **22**, 44 (1974); T. Ogino and M. Aoki, *Jpn. J. Appl. Phys.* **18**, 1049 (1979); D. Elwell *et al.*, *J. Cryst. Growth* **66**, 45 (1984).
6. J. W. Hwang *et al.*, *Chem. Mater.* **7**, 517 (1995); J. E. Andrews and M. A. Littlejohn, *J. Electrochem. Soc.* **122**, 1273 (1975).
7. J. B. Wiley and R. B. Kaner, *Science* **255**, 1093 (1992).
8. J. C. Fitzmaurice and A. Hector, *Polyhedron* **13(2)**, 235 (1994).
9. J. C. Bailer, Ed. *Inorganic Syntheses* (McGraw-Hill, New York, 1955), vol. 4, p. 1.
10. H. S. Booth, Ed., *Inorganic Syntheses* (McGraw-Hill, New York, 1939), vol. 1, p. 26.
11. P. Perlin, C. J. Carillon, J. P. Itie, A. S. Miguel, *Phys. Rev. B* **45**, 83 (1992).
12. H. P. Maruska and J. J. Tietjent, *Appl. Phys. Lett.* **15**, 327 (1969).
13. B. K. Ridley, *Quantum Process in Semiconductors* (Clarendon Press, Oxford, 1982), pp. 62–66.

14. Supported by the Chinese National Foundation of Natural Science Research.

15 February 1996; accepted 4 April 1996

Experimental Constraints on Recycling of Potassium from Subducted Oceanic Crust

Max W. Schmidt*

Petrological experiments on oceanic crust samples characterize the recycling of potassium from mid-ocean ridge basalts and sediments. Metasomatism could develop directly and continuously from subducted potassium-bearing crust from shallow levels to a maximum depth of 300 kilometers. Phengite (a potassium-rich mica) is the principal potassium host at subsolidus conditions. It transports potassium and water to depths of up to 300 kilometers and could yield over the entire depth range potassium-rich fluids or melts (depending on the specific geotherm), which are likely to constitute one of the primary metasomatic agents for generation of calc-alkaline magmas.

Continental crust is growing mainly through calc-alkaline magmatism, which is related to destructive plate boundaries. Calc-alkaline magmatism from volcanic arcs is generally considered to form through partial melting of the mantle wedge after it has been fluxed with fluids or melts (*1–3*). These metasomatic fluids or melts carry water, potassium, and other large ion lithophile (LIL) elements such as Rb, Ba, Sr, and Th. Concentrations and isotopic compositions of U, Th, Pb, B, and Be in calc-alkaline magmas reflect derivation from subducted oceanic crust and sediments (*1*) and indicate that the metasomatic agent originated from the subducted slab (*4*). A systematic increase of K in volcanic arc magmas is commonly observed with increasing depth of subduction zones below arc volcanoes [the so-called K-depth relation (*5*)]. In most cases, this relationship is accompanied by a systematic increase in the abundance of trace elements such as the light rare earth elements (LREEs), Hf, Zr, Nb, Th, U, and Pb (*6, 7*). In this paper, I use a series of experiments to explain the mechanism for transporting K_2O to depth and to understand the generation of K-rich metasomatic fluids.

I performed 51 experiments on mid-ocean ridge basalts (MORB) and andesite bulk compositions (*8*) (Table 1 and Fig. 1). For experiments at pressures above 4.0 GPa, I used a MA-8 multianvil apparatus. The assemblage was composed of prefabricated pyrophyllite gaskets, MgO-octahedra with an edge length of 18 mm, and a stepped graphite heater. Temperature gradients were 20° to 40°, pressure was accurate to ±4%. For experiments below 4.0 GPa, I used an end-loaded piston cylinder with a full salt assembly. Run times of 24 to 38 hours for the multianvil experiments (relatively high pressures and temperatures) and 200 to 350 hours for the piston cylinder experiments (relatively low pressures and temperatures) were necessary to produce almost homogeneous phases, only garnets preserved cores of relict seed compositions. Run products were analyzed by electron microprobe; the presence of small quantities of melt was determined by secondary electron microscopy.

In MORB, andesite [or greywacke (*8*)] (Fig. 1), the principal K-bearing phase observed at subsolidus conditions was phengite (a white mica). It formed at low pressures (<1.5 GPa) and remained present until 9.5 to 10.0 GPa (750° to 1050°C, Fig. 1). In the experiments, the silica content of

Bayerisches Geoinstitut, 95440 Bayreuth, Germany

*Present address: CNRS-URA10, 5 rue Kessler, 63038 Clermont-Ferrand, France. E-mail: max@opgc.univ-bpclermont.fr

Table 1. Basaltic (KMB) and andesitic (RPR) starting material compositions (*8*) and averages (av) for MORB (*22*) and greywackes (GW) (*23*).

	KMB	av-MORB	RPR	av-GW
SiO_2	50.59	50.53	59.55	66.70
TiO_2		1.56	0.71	
Al_2O_3	18.96	15.27	16.97	13.50
Fe_2O_3	1.81		2.01	1.60
FeO	8.24	10.46	4.10	3.50
MnO			0.11	
MgO	6.93	7.47	3.18	2.10
CaO	10.08	11.49	6.55	2.50
Na_2O	2.90	2.62	2.86	2.90
K_2O	0.49	0.16	2.44	2.00
Total	100.00	99.69	99.36	94.80

phengite increased continuously with pressure from 3.5 Si per formula unit (pfu) (9) (2.5 GPa and 700°C) to 4.0 Si pfu (9.0 GPa and 900°C; Table 2). Phengite approached its compositional limit, that is the maximum Si content of 4 Si pfu, and decomposed with increasing pressure when it could no longer accomodate a further increase in Si. At pressures representing depths greater than 110 km, omphacite (a sodic-calcic clinopyroxene) became an important K host in addition to phengite. Potassium-clinopyroxene component in omphacite increased from <0.5 mol% (2.5 GPa) to as much as 6 mol% at 10.5 GPa (900°C; Table 2); thus, omphacite can incorporate significant amounts of K at great depths in subduction zones (*10*).

When the wet solidus of MORB was achieved with increasing temperature (≈1050°C at 9.0 GPa), phengite disappeared rapidly, resulting in 3 to 5% by volume of a K-rich liquid. Small euhedral newly formed garnets were observed in interstitial melt patches. The wet solidus for K-bearing MORB is located at temperatures 100° to 200°C lower than the wet solidus for synthetic K-free MORB [970° to 1160°C at 4.5 to 6.5 GPa (*11*), Fig. 2]. The experimental results suggest that the solidus of K-bearing MORB is defined by incongruent melting of phengite through the reaction phengite + coesite + omphacite = garnet + melt. Experiments on metapelites (*12*) and greywackes indicate that this subsolidus reaction also occurs in these compositions in that subsolidus assemblages are identically phengite + coesite + omphacite + garnet.

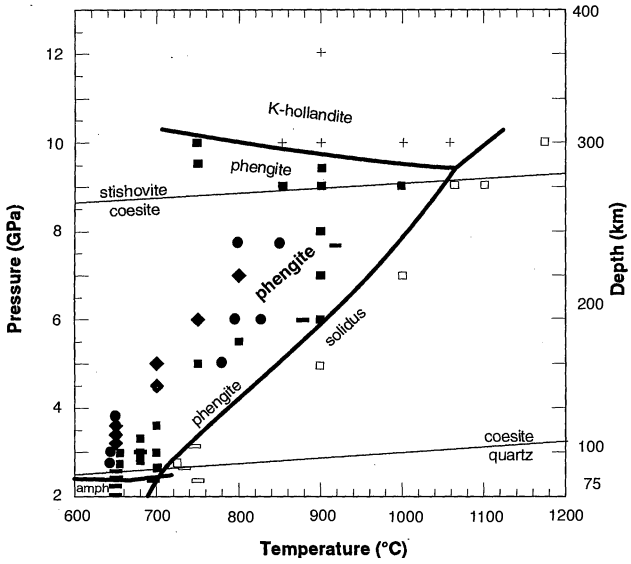

Fig. 1. Pressure-temperature diagram of experiments on basaltic (diamonds, quadrangles, and crosses) and andesitic (circles and horizontal bars) compositions. All filled symbols represent phengite, circles and diamonds indicate lawsonite also present, and open symbols indicate liquid. Experiments at 650°C from (*16, 18*). Assemblages all include garnet, clinopyroxene, and at subsolidus conditions an SiO_2 phase.

Table 2. Mean values of microprobe analyses of experimental products from MORB bulk composition (*24*). *P*, pressure; *T*, temperature.

	Phengites				Omphacites			K-hollandite
P (GPa)	5.5	7.0	7.0	9.0	7.0	9.5	10.5	10.5
T (°C)	800	800	900	900	800	900	900	900
SiO_2	54.08	58.84	56.43	59.62	56.37	56.71	55.86	63.11
Al_2O_3	22.87	15.98	18.94	12.20	12.35	9.26	9.91	19.20
Fe_2O_3					0.00	0.17	0.39	0.00
FeO	1.57	1.69	1.80	3.65	2.29	5.62	5.30	0.99
MgO	5.46	7.55	6.57	8.20	8.88	9.65	9.02	1.95
CaO	0.25	0.22	0.17	0.18	12.45	12.41	12.31	0.38
Na_2O	0.12	0.20	0.10	0.14	6.93	4.98	5.36	0.09
K_2O	10.31	10.37	10.86	10.84	0.43	1.08	1.24	14.02
H_2O	4.50	4.51	4.49	4.45				
Total	99.16	99.36	99.37	99.33	99.70	99.88	99.38	99.76
Si	3.606	3.907	3.765	4.014	1.989	2.027	2.010	2.923
Al	1.797	1.251	1.489	0.968	0.514	0.390	0.420	1.049
Fe^{III}					0.000	0.004	0.011	0.000
Fe^{II}	0.088	0.094	0.100	0.206	0.068	0.168	0.159	0.038
Mg	0.542	0.748	0.654	0.823	0.467	0.514	0.484	0.135
Ca	0.018	0.016	0.013	0.013	0.471	0.475	0.475	0.019
Na	0.016	0.025	0.013	0.019	0.474	0.345	0.374	0.008
K	0.877	0.879	0.925	0.931	0.019	0.049	0.057	0.828
H	2.000	2.000	2.000	2.000				
Σcations	6.944	6.920	6.959	6.974	4.000	3.972	3.990	5.000

The subduction history of highly soluble elements such as potassium is directly related to fluid content. In nature, fluid saturation is to be expected because dehydration reactions liberate fluid during prograde metamorphism. However, the quantity of free fluid phase present in the descending oceanic crust is expected to be small (in fluid inclusions and intergranular fluids), and most of the fluid will ascend. Experimentally, the natural situation is best simulated with low fluid contents sufficient to saturate the system but with only a small quantity of free fluid (*13*). I thus performed experiments with 1, 2, or 5% H_2O per weight. At pressures above the phengite breakdown (>10.0 GPa), experiments with low H_2O content (1% by weight) yielded almost pure $KAlSi_3O_8$ (K-hollandite structure; Table 2) instead of phengite. In experiments with more than 1% H_2O by weight, K-hollandite or any other solid K-bearing equilibrium phase was not observed as a breakdown product of phengite. Instead, submicrometer to 10 μm K-bearing silicate phases appeared abundantly at grain boundaries between garnet and clinopyroxene. These phases obviously precipitated from the fluid phase. This observation indicates that K was strongly partitioned into the fluid phase and is interpreted as evidence of the breakdown of phengite to omphacite + garnet and a K-rich fluid (*14*).

The experiments show that phengite, and at higher pressure K-hollandite and also omphacite, can carry K to great depths in subduction zones, but that any fluid resulting from phengite breakdown will be strongly enriched in K (and other mobile elements such as Rb, U, Pb, and B). Consequently, fluids passing through, or arising from, subducted oceanic crust at great depth may leach some of the K from this crust during prograde metamorphism.

Tatsumi (*2, 7*) proposed that descending oceanic crust released all its potassium when amphibole broke down at ~2.5 GPa. This release led to subsequent metasomatism of the overlying mantle wedge and transportation of K_2O through mantle phases such as phlogopite or K-richterite. My experiments suggest an alternative mechanism for burying K_2O in subduction zones. Minor amounts of K-rich sediments and abundant K-poor hydrated basaltic and gabbroic crust will lose a small

amount of K into fluids generated during initial partial dehydration at shallow levels (<10 km). Blueschists represent a part of the slab that was subducted beyond conditions of such low-temperature alteration. These rocks document that the descending crust still contains 3 to 6% H_2O by weight at depth of 10 to 50 km and that an essentially unchanged bulk chemistry with regard to their protoliths is maintained (*15*); a substantial loss of potassium did not occur during low-T alteration. In blueschists, most K present is contained in phengite (*15*). At greater depth, phengite coexists with sodic-calcic amphibole (*16*), which contains only minor amounts of K [≤0.3% in weight (*16*)]. Thus, at 2.5 Gpa, most of the K is still stored in phengite and K and also H_2O is carried to depths in excess of the amphibole breakdown [70 to 75 km (*16–18*) at temperatures of 550° to 700°C]. The presence of minor amounts of phengite in metabasalts and major amounts of phengite in metasediments from eclogite terraines where coesite was reported (*19*) documents that K is retained in subducted crust to conditions beyond depths of 90 km. For depths of 75 to 300 km, mass balance calculations based on experimental mineral compositions reveal that with increasing pressure during subduction, omphacite (40 to 55% by volume) could store almost all potassium present in a MORB bulk composition. Thus, the final phengite breakdown at depths of 300 km would release only minor K and H_2O in MORB. However, from 100 to 300 km, when K-omphacite forms continuously from phengite through the reaction phengite = $KAlSi_2O_6$-clinopyroxene + enstatite + coesite + K-rich fluid, K will be continuously released from the subducted crust through solution in fluids. In contrast to MORB bulk compositions, pelites (*12*) or greywackes with higher K_2O contents (1.4 to 4% by weight) and lower omphacite abundances (20 to 30% by volume) may still have significant amounts of phengite (10 to 35% by volume) at 300 km depth (10 GPa). Thus a pulse of K-rich fluid is generated in sediments at depths of ~300 km when K-hollandite + K-rich fluid form from phengite. At greater depths, the descending crust is almost completely dehydrated and should not cause further K-metasomatism.

The mechanism described above applies to subduction zones where thermal conditions remain in the subsolidus region. For hot subduction zones (*3*, *20*) it appears that the solidus is reached at depths between the amphibole breakdown and the phengite stability limit, that is, between 70 and 300 km (Fig. 2). In such a case, phengite melts incongruently and generates K-rich melt. This melt could metasomatize the overlying mantle wedge. The exact depth of this melting process depends on the specific geotherm of an individual subduction zone.

At blueschist conditions, phengite is the principal host of Rb, Ba, B, and Be (*21*). Be, B, and Pb isotopes show that calc-alkaline arc magmas have a crustal component dominated by altered MORB (mixed with minor sediments) (*4*). A relative increase of K and LIL elements in the crustal component of arc magmatism with increasing depth could be explained by the role of phengite relative to other hydrous phases during dehydration or melting of subducted crust [a similar model has been deduced from geochemical arguments (6)]. At shallow to intermediate depths (<110 km) the fluid production history of subducted oceanic crust is dominated by dehydration of K-free phases such as chlorite, epidote or zoisite, lawsonite, amphibole, and chloritoid (*18*). At larger depths, phengite is the dominant hydrous phase in subducted crust [in extremely cold subduction zones lawsonite also occurs (*18*); Fig. 2], and thus controls the dehydration or melting process at depths larger than 110 km (Fig. 2). As a consequence, metasomatism generated from oceanic crust in large depth is expected to be enriched in K.

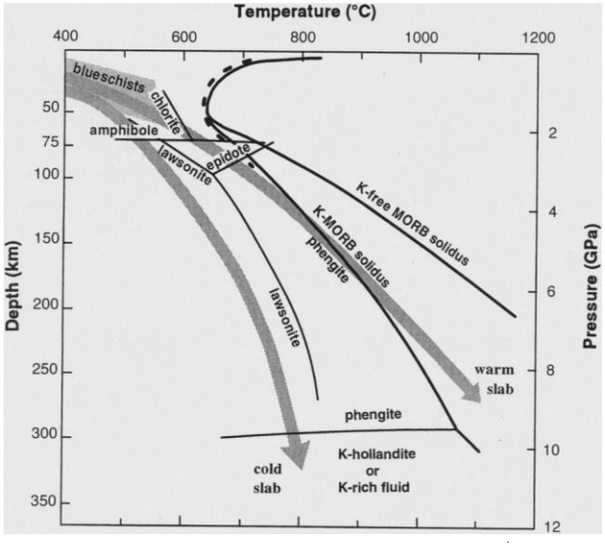

Fig. 2. Phase relationships and dehydration paths of subducting lithosphere. Typical pressure-temperature paths for cold and warm subduction zones are shown (*3*, *20*, *25*). Solidus for basalt at pressures below 2.0 GPa from (*26*); amphibole, chlorite, epidote/zoisite and lawsonite phase boundaries from (*18*). Solidus for metapelite from (*27*) (stippled line). At depths greater than 110 km, melting in basalts, greywackes, and metapelites occurs through the same solidus reaction at similar pressure-temperature conditions (see text). In extremely cold subduction zones lawsonite (*18*) and phengite will be stable to 300 km, at intermediate conditions, only phengite persists to 300 km. In warm subduction zones, oceanic crust will melt between 70 and 300 km because the solidus reaction is almost parallel to possible pressure-temperature paths, small differences in thermal structure will cause large differences in melting depth. As can be seen from this diagram, individual subduction zones will have very different phase assemblages during dehydration and different pressure-temperature conditions of final dehydration or melting as a function of the thermal regime.

REFERENCES AND NOTES

1. M. R. Perfit, D. A. Gust, A. E. Bence, R. J. Arculus, S. R. Taylor, *Chem. Geol.* **30**, 227 (1980).
2. Y. Tatsumi, *J. Geophys. Res.* **94**, 4697 (1989).
3. J. H. Davies and D. J. Stevenson, *ibid.* **97**, 2037 (1992).
4. J. D. Morris, W. P. Leeman, F. Tera, *Nature* **344**, 31 (1990); T. Ishikawa and E. Nakamura, *ibid.* **370**, 205 (1994); T. Plank and C. H. Langmuir, *ibid.* **362**, 739 (1993); O. Sigmarsson, M. Condomines, J. D. Morris, R. S. Harmon, *ibid.* **346**, 163 (1990).
5. W. R. Dickinson and T. Hatherton, *Science* **157**, 801 (1967); W. R. Dickinson, *Geology* **3**, 53 (1975).
6. I. A. Nicholls, D. J. Whitford, K. L. Harris, S. R. Taylor, *Chem. Geol.* **30**, 177 (1980).
7. T. Tatsumi and S. Eggins, *Subduction Zone Magmatism* (Blackwell, Cambridge, 1995), pp. 80–99.
8. In order to produce higher abundances and thus larger crystals of phengite I studied a K-enriched MORB. The phase relationships determined for andesite are also valid for greywackes, they have similar major element compositions. The lower calcium content of greywackes with respect to andesites will result in a slightly lower epidote and lawsonite stability in greywackes. Starting materials were constituted by mixtures of synthetic glass ($Fe^{3+}/Fe^{(tot)}$ = 0.2) and 20% crystal seeds (equal parts of grossular, almandine, jadeite, diopside, and zoisite) and some $Al(OH)_3$. $Al(OH)_3$ allows for addition of precise amounts of H_2O to the starting material (1%, 2% and 5% by weight) avoiding any evaporation of H_2O during welding of the small (2.0 by 2.0 mm) Au capsules.
9. Phengite belongs to the muscovite-celadonite solid solution $(KAl_2[AlSi_3]O_{10}(OH)_2$-$KMgAl[Si_4]O_{10}(OH)_2)$, its main compositional variable is the silica content (Si pfu). Silica contents of phengite are commonly used as geobarometer (*14*) in natural eclogites, typically ranging from 3.15 to 3.5 Si pfu.
10. Natural high-K clinopyroxenes are reported from diamond + phengite bearing eclogites from Kasachstan (N. V. Sobolev and V. S. Shatsky, *Nature* **343**, 742, 1990). Clinopyroxene with high K contents are also reported in K_2O-solubility studies on synthetic jadeite and diopside (G. E. Harlow, *Geol. Soc. Am. Abstr. Prog.* **24**, 129, 1992).
11. R. J. Sweeney and A. B. Thompson, *Terra Abstr.* **7**, suppl. no. **1**, 145 (1995).
12. K. J. Domanik and J. R. Holloway, *Eos* **75**, 744, (1994).
13. Experiments from the 1960s and 1970s were commonly performed with water contents of 20 to 50% by weight. Such experiments [for example, I. B. Lam-

bert and P. J. Wyllie, *J. Geol.* **82**, 88 (1974)] were not designed to investigate the stabilities of K-bearing phases and often resulted in a complete dissolution of K in the fluid phase.
14. See also H. J. Massone and W. Schreyer, *Contrib. Mineral Petrol.* **96**, 212 (1987).
15. B. W. Evans and E. H. Brown, Eds., *Geól. Soc. Am. Mem. 164* (1986).
16. M. W. Schmidt, *Am. J. Sci.* **293**, 1011 (1993).
17. S. Poli, *ibid.* **293**, 1061 (1993).
18. _____ and M. W. Schmidt, *J. Geophys. Res.* **100**, 22299 (1995).
19. Phengite coexisting with coesite is reported from mafic eclogites in Norway [D. C. Smith, in *Eclogites and Eclogite-Facies Rocks*, D. C. Smith, Ed. (Elsevier, Amsterdam, 1988), pp. 1–206] and Dabie Shan, China [R. Y. Zhang and J. G. Liou, *Eur. J. Mineral.* **6**, 217 (1994)], and from metasedimentary eclogites from Dora Maira, Italy [C. Chopin, *Contrib. Mineral. Petrol.* **86**, 107 (1984)], and Zermatt-Saas zone, Switzerland/Italy [T. Reinecke, *Eur. J. Mineral.* **3**, 7 (1991)].
20. M. N. Toksöz, J. W. Minear, B. R. Julian, *J. Geophys. Res.* **76**, 1113 (1971); Y. Furukawa, *ibid.* **98**, 8309 (1993); S. M. Peacock, *Science* **248**, 329 (1990).
21. K. J. Domanik, R. L. Hervig, S. M. Peacock, *Geochim. Cosmochim. Acta* **57**, 4997 (1993).
22. W. G. Melson, T. M. Vallier, T. L. Wright, G. Byerly, J. Nelen, *J. Am. Geophys. Union Trans.* **4**, 351 (1976).
23. F. J. Pettijohn, *U.S. Geol. Surv. Prof. Pap. 440-S*, (1963).
24. Analyses were performed with an electron beam sufficiently defocused to avoid K and Na loss. Phengite analyses are normalized to 12 oxygens including 2 OH-groups, all Fe as Fe^{2+}. Note that deviations from the ideal muscovite-celadonite solid solution appear.
25. A. B. Thompson, *Nature* **358**, 295 (1992).
26. I. B. Lambert and P. J. Wyllie, *J. Geol.* **80**, 693 (1972).
27. G. T. Nichols, P. J. Wyllie, C. R. Stern, *Nature* **785**, 785 (1994).
28. I thank S. Poli and O. Sigmarsson for discussions and D. Rubie for financial support.

1 February 1996; accepted 10 April 1996

Pore Fluid Constraints on the Temperature and Oxygen Isotopic Composition of the Glacial Ocean

Daniel P. Schrag, Gretchen Hampt, David W. Murray

Pore fluids from the upper 60 meters of sediment 3000 meters below the surface of the tropical Atlantic indicate that the oxygen isotopic composition ($\delta^{18}O$) of seawater at this site during the last glacial maximum was 0.8 ± 0.1 per mil higher than it is today. Combined with the $\delta^{18}O$ change in benthic foraminifera from this region, the elevated ratio indicates that the temperature of deep water in the tropical Atlantic Ocean was 4°C colder during the last glacial maximum. Extrapolation from this site to a global average suggests that the ice volume contribution to the change in $\delta^{18}O$ of foraminifera is 1.0 per mil, which partially reconciles the foraminiferal oxygen isotope record of tropical sea surface temperatures with estimates from Barbados corals and terrestrial climate proxies.

Pleistocene oxygen isotope records of foraminifera in deep sea sediments reflect changes in ocean temperature and in the oxygen isotopic composition of seawater ($\delta^{18}O_{sw}$) over glacial cycles. Cooling during glacial episodes increases the mass-dependent fractionation of oxygen isotopes between water and calcite, resulting in higher $\delta^{18}O$ values of carbonate microfossils. The growth of large ice sheets on continents increases the $^{18}O/^{16}O$ ratio of seawater, also resulting in higher $\delta^{18}O$ values for carbonate microfossils. Determining how much each of these components contributes to the total change in $\delta^{18}O$ of foraminifera since the last glacial maximum (LGM), which for benthic foraminifera averages 1.7 per mil (*1*), is an important step toward understanding Pleistocene climate change.

The generally accepted estimate for the contribution of ice volume to the change in $\delta^{18}O$ of foraminiferal calcite is 1.3 per mil (*2*, *3*), which implies that the deep ocean was 2°C cooler during the LGM. We suggest a revision of this estimate based on measurements of deep sea pore fluids using a method presented by Schrag and DePaolo (*4*). The change in $\delta^{18}O_{sw}$ caused by changes in continental ice volume through the Pleistocene represents a periodic boundary condition for the sediment–pore fluid system. This variation diffuses down from the sea floor, leaving a profile of $\delta^{18}O$ versus depth in the pore fluid that is a record of the $\delta^{18}O$ history of the overlying seawater. The $\delta^{18}O_{sw}$ during the LGM can be reconstructed with the use of a numerical model to calculate the attenuation of the signal as long as high-precision, high-resolution pore fluid data are available.

Pore fluids were sampled during Leg 154 of the Ocean Drilling Program (ODP) from Site 925, drilled at a water depth of 3041 m on the Ceara Rise (4°12′N, 43°29′W) (*5*). The oxygen isotope data (*6*) identify a peak in $\delta^{18}O$ between 20 and 35 m below the sea floor (Fig. 1). The $\delta^{18}O$ values are constant at −0.02 per mil in the first 7 m. From 10 to 20 m, the $\delta^{18}O$ values increase to 0.18 per mil, followed by a plateau from 20 to 35 m. Below 35 m, the $\delta^{18}O$ values decrease to a minimum of −1.75 per mil at a depth of 569 m.

We modeled the data by using the periodic change in $\delta^{18}O_{sw}$ with time at the sediment-water interface given by benthic $\delta^{18}O$ records for ODP Site 677 (*7*) and Core V19-30 (*8*). We assumed that the relative contributions of temperature and $\delta^{18}O_{sw}$ to the benthic $\delta^{18}O$ records were constant with time and adjusted the amplitude of those records in multiple calculations with glacial-interglacial changes in $\delta^{18}O_{sw}$ of 0.7, 1.0, and 1.3 per mil. The decrease in $\delta^{18}O_{sw}$ over the last 20,000 years was calculated from the Barbados sea level curve (*2*, *9*). The effects of sedimentation (~30 cm per 1000 years at Site 925) and chemical reaction were not considered because they are too slow over the time period to affect the calculations. We used diffusion coefficients from measured values of the self-diffusion of water (*10*) (adjusted for tortuosity using the square of the measured porosity) and a bottom-water temperature of 3°C (*11*). The diffusion coefficient

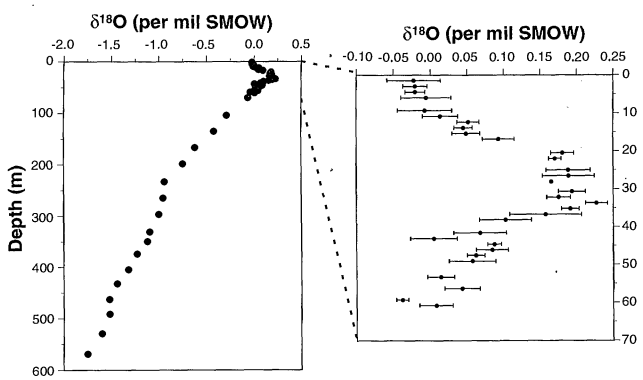

Fig. 1. Oxygen isotope data on pore fluids [relative to standard mean ocean water (SMOW)] from Site 925, plotted versus depth. Error bars for data in the upper 60 m represent one standard deviation of four replicate measurements.

D. P. Schrag, Department of Geological and Geophysical Sciences, Princeton University, Princeton, NJ 08544–1003, USA.
G. Hampt, Institute of Marine Sciences, University of California, Santa Cruz, CA 95064, USA.
D. W. Murray, Department of Geological Sciences, Brown University, Providence, RI 02912, USA.